Microscopic and Quantitative Investigations on PST Ti-Al / Ti Reaction Diffusion Couples

Ling Pan, David E. Luzzi
Department of Materials Science and Engineering, University of Pennsylvania
3231 Walnut Street, Philadelphia, PA 19104, U.S.A.

ABSTRACT

Interdiffusion in multi-phase diffusion couples of polycrystalline Ti and polysynthetically twinned (PST) Ti-49.3 at.% Al, with the diffusion direction parallel to the lamellar planes, is investigated in the temperature range 973 – 1173 K. A reaction zone (RZ) of the α_2-Ti_3Al phase forms between the end materials and exhibits deeper penetration in the α_2 lamellae than in the primary γ lamellae. The mass balance and the lamellar thickness across the RZ / PST interface are believed to be the major factors that lead to the different behaviors in the penetration depth of the RZ. Direct measurements of the RZ thickness reveal a parabolic growth of the RZ, indicating a diffusion-controlled growth macroscopically. Concentration profiles from the Ti, through the RZ, into the PST γ and α_2 lamellae are measured by x-ray spectroscopy in a transmission electron microscope. Deviations from a diffusion-controlled composition profile indicate some extent of interface-controlled growth. Plateaus are seen in the concentration profiles in the RZ adjacent to the RZ/PST interface, extending through most of the deeply penetrated well region. The interfacial energy and strain energy are possible reasons for the plateaus. The interdiffusion coefficients are found to be largely independent of composition with a temperature dependence that obeys the Arrhenius relationship.

INTRODUCTION

Titanium aluminide based intermetallic alloys have great potential in high temperature structural applications in aerospace and automotive industries [1-2]. Mechanically superior alloys of this system usually have a two-phase lamellar structure of γ-TiAl and α_2-Ti_3Al. In the past decade, special interest has been paid to so-called polysynthetically twinned (PST) Ti-Al, composed of alternate lamellae of γ-TiAl and α_2-Ti_3Al with the orientation relationship $\{111\}_g \,//\, (0001)_{a_2}$ and $\langle 1\bar{1}0\rangle_g \,//\, \langle 11\bar{2}0\rangle_{a_2}$ [3]. Diffusion plays an important role in the formation and high-temperature stability of the lamellar structure. Furthermore, diffusion is an essential determinant of some mechanical properties, such as creep resistance. Therefore, a fundamental understanding of the diffusion mechanisms in PST Ti-Al alloys is of great importance for the development of titanium aluminide alloys.

There has been a large amount of tracer diffusion data available in Ti-Al system [4-8]. However, tracer diffusion experiments measure the average layered concentration profile. The technique cannot distinguish the effects of each individual phase and of the various types of interfaces in a PST crystal on diffusion. Little has been known about the fundamental correlation between the microstructure and diffusion properties, especially in reactive interdiffusion cases.

In the present paper, we present the microscopic and quantitative results in multi-phase diffusion couples of Ti and PST Ti-Al crystal. The more detailed microstructural evolution and the interdiffusion results have been reported in two separate papers, respectively [9-10].

EXPERIMENTAL PROCEDURES

PST Ti-49.3 at.% Al crystals were grown in an ASGAL optical floating zone furnace under flowing argon gas with a growth rate of 3 mm/h. Slices parallel to the $\{1\bar{1}0\}$ planes, about 0.5 mm thick, which were perpendicular to the lamellar planes, were cut from the as-grown PST crystals. The directions mentioned here and after refer to the γ-TiAl phase in the PST crystal. Without losing generality, we assume that the lamellar planes in the γ phase are (111). Prior to diffusion bonding, the slices of the PST crystals were mechanically and electrolytically polished, and the bulk Ti (99.999%) specimens were mechanically polished using an Allied High Tech MultiPrep polisher to ensure the parallelism. Diffusion couples of PST Ti-Al and Ti were produced by diffusion bonding in a high vacuum hot-pressing furnace at 600°C for two hours. No extra mechanical stress was applied to the material during diffusion bonding except that from the thermal expansion of the graphite rams. Cross-sections of the as-bonded diffusion couples were cut perpendicular to both the bonding plane and the lamellar interfaces of the PST crystal, i.e. in the $<11\bar{2}>$ direction, and were observed with a JEOL 6400 scanning electron microscope (SEM) operated at 15 kV. The as-bonded diffusion couples were subjected to diffusion anneals in the same furnace at temperatures 650, 700, 750, 800, 850 and 900°C for various times. For each diffusion couple, a series of consecutive diffusion-anneals were carried out at the same temperature to elucidate the diffusion kinetics.

Transmission electron microscopy (TEM) specimens were cut from the annealed diffusion couples using a Strata DB 235 dual beam focused ion beam (FIB) system at Lehigh University. Thin foils for TEM analysis were prepared with foil normals near to $<11\bar{2}>$, [111] and <110>. Most observations, including all in this paper, were made on foils with the $<11\bar{2}>$ orientation. TEM specimens were examined in a JEOL 2010F TEM operated at 200 kV. Energy dispersive x-ray spectroscopy (EDS) in the scanning transmission electron microscopy (STEM) mode of the 2010F was used to measure the chemical composition profiles of the diffusion couples. A TEM specimen was prepared from a bulk polycrystalline Ti-34 at.% Al (α_2-Ti_3Al single phase) sample as a standard. The quantitative chemical analysis utilizes the Cliff-Lorimer ratio technique [11].

RESULTS AND DISCUSSIONS

A reaction layer or reaction zone (RZ) with wavy contour in the PST Ti-Al side emerges at the bonding interface after annealing and its thickness increases with annealing time. Electron diffraction patterns in TEM have verified that it is the α_2-Ti_3Al phase, which follows from the equilibrium phase diagram. To elucidate the growth kinetics of the reaction layer, SEM observations and measurements on back scattered electron images were carried out on the bulk diffusion couples after each anneal. Figure 1 shows a typical SEM back scattered electron image of a diffusion couple after an anneal at 650°C for eight hours. The upper white part is the polycrystalline Ti and the lower lamellar structure is the PST crystal, with the gray vertical thin laths the α_2-Ti_3Al lamellae and the majority dark lamellae the γ-TiAl phase. The light gray layer between the Ti and the PST lamellae is the so-called RZ. Several interesting features are present in this image. First, the α_2-lamellae tend to group with some fine γ lamellae. Second, the RZ exhibits a clear contrast difference with both phases of the PST Ti-Al, indicating an abrupt composition change across the RZ/PST interface. Third, the penetration depth of the RZ into the γ lamellae is in general smaller than that into the α_2 lamellae.

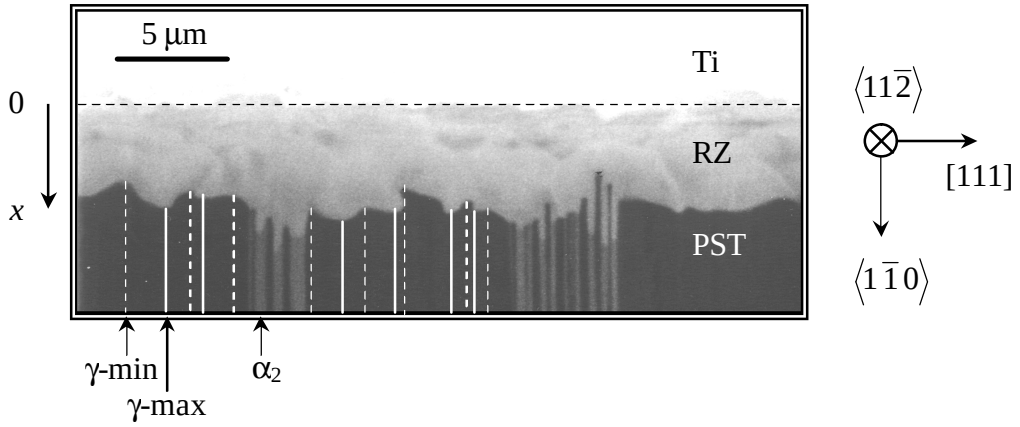

Figure 1. Illustration of the measurements of the RZ thickness on SEM back scattered electron images of PST-Ti diffusion couple annealed at 650°C for 8 hours after bonding.

The clear contrast difference in the SEM back-scattered electron images between the RZ and the PST crystal allows a direct measurement of the thickness of the RZ. A series of SEM back-scattered electron images were recorded over a continuous region to form a map of each diffusion couple at each annealing condition. Since the RZ/Ti interface is mostly straight, a line across the interface of the RZ and Ti through the images is drawn and regarded as the zero-thickness level of the RZ, as illustrated in figure 1. The thickness of the RZ, *x*, was measured at each point where the RZ exhibited local minima or maxima in thickness adjacent to the γ-TiAl lamellae, categorized as γ-min and γ-max, respectively. In order to obtain the net increase of *x* corresponding to each individual annealing period, the average RZ thickness of the as-bonded diffusion couples was subtracted from the measurements in the annealed diffusion couples. Hundreds of measurements were made and averaged for both categories. The growth of the reaction layer is then illustrated by plotting x^2 versus *t* at each temperature, as shown in figure 2. It is revealed that *x* increases parabolically with the annealing time *t*, which indicates that the growth of the α_2-Ti_3Al phase in the RZ is mainly diffusion-controlled at a macroscopic level.

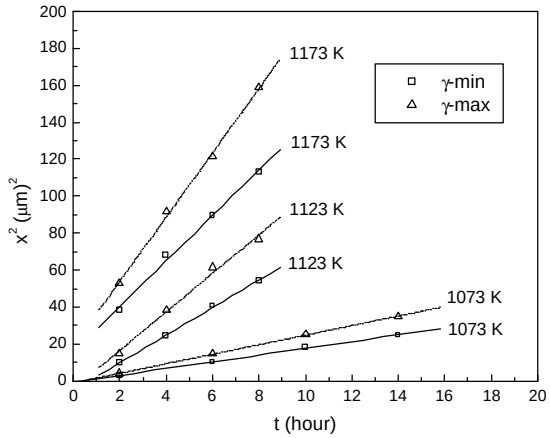

Figure 2. The parabolic growth of the reaction layer at various temperatures.

A typical TEM bright field image of a diffusion couple annealed at 1173 K for two hours is shown in figure 3(a), with the beam direction ***B*** = <1$\bar{1}$0> and the lamellar planes edge on. The

interface types between the individual γ lamellae were determined by electron diffraction and are labeled — OT: ordinary twin, RF: rotational fault, PT: pseudo-twin. The penetration depth of the RZ into the α_2 lamella is much deeper than that in the γ lamellae, forming a well-like structure, which is consistent with the SEM observation. This deeper penetration in the mixed α_2 lath than in primary γ lamellae is mostly a result of mass balance [9]. At the sidewalls of the well formed by the deeply penetrated RZ grain in the original mixed α_2 lath in figure 3(a), the interfaces between the RZ grain and the neighboring primary γ lamellae exhibit small angles with the lamellae, which is evidence of lateral lattice diffusion assisted RZ grain growth across the lamellae. It is obvious that the RZ grain growth across the lamellae is much less than the growth parallel to the lamellae. This is associated with the close-packed structure of the lamellar planes. The activation energy for the atoms crossing a close-packed plane is usually high. As a result, the RZ grain growth across the lamellae likely occurs through a ledge mechanism, which is consistent with the high resolution electron microscopy (HREM) observations [9]. An enlarged image of the area enclosed by the rectangular box in figure 3(a) is shown as figure 3(b). As can be seen, the thick α_2 lamella consists of a set of finer lamellar structures. HREM was used to determine that the α_2 lamella is actually composed of much finer γ and α_2 lathes with thickness of 10-150 nm [9]. This was a common observation for other thick α_2-Ti_3Al lamellae seen in other TEM specimens. The fine γ lamellae presumably formed by secondary precipitation within the thick α_2 lamellae during directional solidification of the PST crystal. For the ease of description, we shall denote this group of fine mixed phase lamellae as a “mixed α_2 lath”.

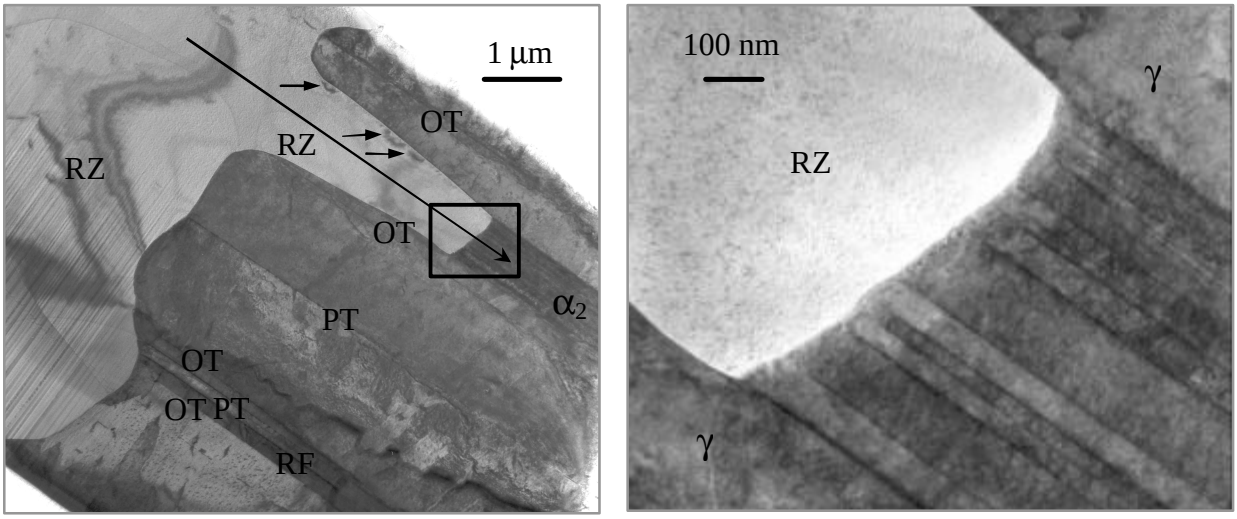

Figure 3. Bright field TEM images of a diffusion couple that was annealed at 1173 K for two hours with $\boldsymbol{B} = <1\bar{1}0>$ and the lamellar planes edge on. (b) is the magnified images of the area enclosed by the rectangular box in (a).

Concentration profiles were measured along the diffusion direction parallel to the lamellae with the lamellar planes edge on, from Ti, through the RZ, into both the mixed α_2 lath and the primary γ lamellae of the PST crystal, as indicated by the long arrow along the deeply penetrated RZ grain in figure 3(a). Figure 4 provides an example of the concentration profiles measured on

the same specimen from the RZ into a secondary γ lamella in the mixed α_2 lath of the PST crystal and from the RZ into the two primary γ lamellae adjacent to this mixed α_2 lath. As illustrated by the schematic diagram of figure 4, the solid, dashed and dotted vertical lines in the concentration profiles indicate the interfaces between the RZ and secondary γ, primary γ1 and primary γ2 lamellae, respectively. As expected from the phase diagram, there are sharp discontinuities in composition across the RZ/γ interfaces. A plateau in composition in the RZ adjacent to the RZ/PST interface is also present and extends through most of the deeply penetrated well region, as observed in other specimens [10]. In addition, it can be seen that although the penetration depth of the RZ into the primary γ lamellae and the mixed α_2 lath varies, the compositions at the same depth in the RZ are about the same regardless of their relative positions with respect to the lamellae.

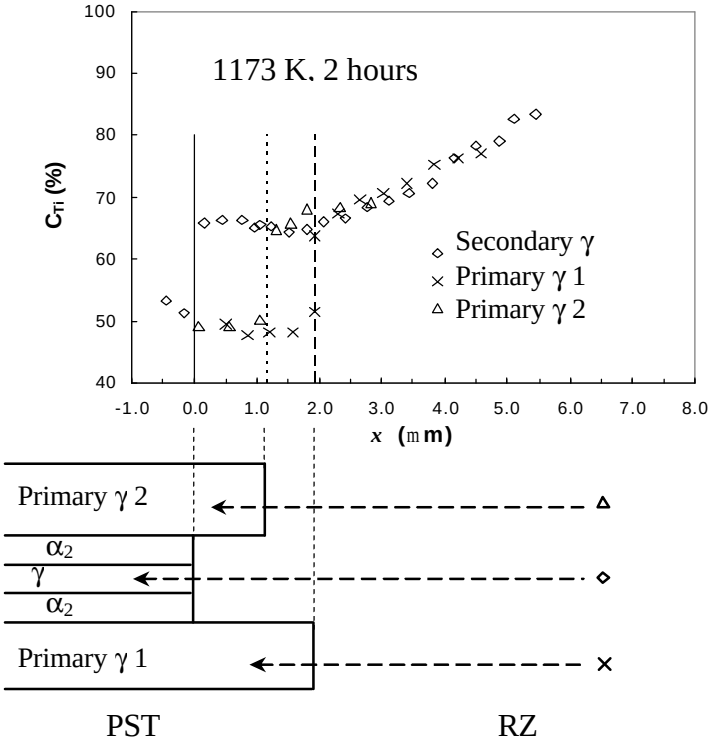

Figure 4. Concentration profiles from the RZ to a secondary γ lamella in the mixed α_2 lath and two primary γ lamellae of the diffusion couple annealed at 1173 K for two hours.

The discontinuity in composition at the RZ/α_2(PST) interface is an indication of the role of some extent of interface-controlled growth of the RZ. A possible explanation is that the RZ grain forms some arbitrary coherent or semicoherent boundary with the γ-TiAl lamellae while forming a high-angle GB with the α_2 lamellae [9]. Therefore, the low mobility of the (semi)coherent boundary provides a barrier for the atoms to cross the boundary. The origins of the plateau in the diffusion profile are not quite clear. Since the plateau occurs in the deeply penetrated RZ well region, the following explanations are proposed. Increased interfacial energy and strain energy in the deeply penetrated well area that result from the phase transformation are proposed as the underlying cause for the plateau. The presence of this increased energy state is evident from the bend contours present in figure 3(a), marked by the small arrows, which are indications of the structural strain due to the incoherent RZ/(primary γ) interface at the sidewall of the well [10].

The interdiffusion coefficient is evaluated both independent of composition and as a function of composition [10]. No significant concentration dependence of the interdiffusion coefficients is observed using Boltzmann-Matano analysis. The temperature dependence of the interdiffusion coefficients obeys the Arrhenius relationship with a pre-exponential factor of $D_0 = (7.56 \pm 7.14) \times 10^{-5}\ m^2/s$ and an activation enthalpy of $Q = \left(255.6^{+8.9}_{-8.3}\right) kJ/mol$ [10].

CONCLUSIONS

In diffusion couples of Ti and PST Ti-Al, a reaction zone of polycrystalline α_2-Ti_3Al forms between the end materials and exhibits deeper penetration in α_2 lamellae than in primary γ lamellae. Most of the α_2 lamellae are composed of much finer secondary γ and α_2 lamellae. The mass balance and the lamellar thickness across the RZ / PST interface are believed to be the major factors that lead to the different behaviors in the penetration depth of the RZ. Direct measurements of the RZ thickness reveal a parabolic growth of the RZ, indicating a diffusion-controlled growth at a macroscopic level. Deviations from a diffusion-controlled concentration profile indicate some extent of interface-controlled growth. Plateaus are seen in the concentration profiles in the RZ adjacent to the RZ/PST interface, extending through most of the deeply penetrated well region. The interfacial energy and strain energy are possible reasons for the plateaus. The interdiffusion coefficients are found to be largely independent of composition with a temperature dependence that obeys the Arrhenius relationship.

ACKNOWLEDGEMENT

The authors thank Mr. David Ackland at Lehigh University for using their FIB equipment to prepare the TEM specimens. This research was supported by National Science Foundation grant no. DMR96-15228. This work benefited from access to the Penn Regional Materials Characterization facility, partially supported through the Penn NSF MRSEC grant no. DMR 00-79909 and used the JEOL 2010F FE-TEM acquired with NSF support no. DMR 94-13550.

REFERENCES

1. F. H. Froes and C. Suryanarayana, in *Physical Metallurgy and Processing of Intermetallic Compounds*, N. S. Stoloff and V. K. Sikka, ed., Chapman & Hall, New York, 1996, Chapter 8.
2. S. C. Huang and J. C. Chesnutt, in *Intermetallic Compounds:* Vol. 2, *Practice*, J. H. Westbrook and R. L. Fleischer, ed., John Wiley & Sons, 1994, Chapter 4.
3. M. J. Blackburn, in *The Science, Technology and Application of Titanium*, Eds. R. I. Jaffee and N. E. Promisel, Pergamon, London (1970) 633.
4. Chr. Herzig, T. Przeorski and Y. Mishin, *Intermetallics* **7** (1999) 389.
5. J. Rüsing and Chr. Herzig, *Intermetallics* **4** (1996) 647.
6. S. V. Divinski, F. Hisker, A. Bartels and Chr. Herzig, *Scripta Mater*. **45** (2001) 161.
7. W. Sprengel, N. Oikawa and H. Nakajima, *Intermetallics* **4** (1996) 185.
8. Chr. Herzig, T. Wilger, T. Przeorski, F. Hisker, S. Divinski, *Intermetallics* **9** (2001) 431.
9. L. Pan and D. E. Luzzi, submitted.
10. L. Pan and D. E. Luzzi, to be submitted.
11. G. Cliff and G. W. Lorimer, *J. Micros.* **103** (1975) 203.